

OVERVIEW

Earlier studies using coupled atmosphere-ocean climate models show that heavy and extreme precipitation increases over much of North America in a future warmer climate, (e.g., Sun et al. 2007, Tebaldi et al. 2006). Proposed mechanisms for the increases in extreme precipitation include increases in atmospheric water vapor (e.g., Allen and Ingram 2002), changes in convective updrafts that produce extreme precipitation (e.g., O’Gorman and Schneider 2009), and changes in the atmospheric circulation patterns associated with extreme daily events (e.g., Wehner 2012). In this poster, we study changes in daily heavy and extreme precipitation between a historical and future climate scenario in the recently available coupled atmosphere-ocean simulations from the Coupled Model Intercomparison Project Phase 5 (CMIP5).

Our results are consistent with earlier studies in that increases in heavy precipitation are largest near the Atlantic and Pacific coasts and at high latitudes, while little change or decreases occur elsewhere. Increases in heavy precipitation at middle and high latitudes are close to what one would expect from increases in atmospheric water vapor. The atmospheric circulation patterns associated with extreme precipitation events do not appear to change significantly in the future over most locations. Additional analysis of the physical mechanisms associated with extreme precipitation events, particularly where extreme precipitation decreases in the future, is warranted.

DATA AND METHODOLOGY

- **Models:** Output (daily resolution) from 24 CMIP5 models (one ensemble member from each).
- **Historical:** Simulation of the recent past including observed changes in atmospheric composition, solar forcing, and land use:
January 1, 1979 – December 31, 1999.
- **RCP85:** Future simulation in which radiative forcing reaches approximately 8.5 W m^{-2} by 2100:
January 1, 2079 – December 31, 2099.
- **Resolution:** A common grid of $2.5^\circ \times 2.5^\circ$ lon-lat is used for analysis, where linear interpolation or area averaging was used in the regridding process.

ACKNOWLEDGEMENTS

- We acknowledge the World Climate Research Programme’s Working Group on Coupled Modelling, which is responsible for CMIP, and we thank the climate modeling groups for producing and making available their model output. For CMIP the U.S. Department of Energy’s Program for Climate Model Diagnosis and Intercomparison provides coordinating support and led development of software infrastructure in partnership with the Global Organization for Earth System Science Portals.
- This work was supported by a fellowship from the Environmental Protection Agency Science to Achieve Results (EPA STAR) program and a grant from the NOAA Climate Program Office.

REFERENCES

- CMIP5 Overview: WCRP Coupled Model Intercomparison Project – Phase 5: Special Issue of the CLIVAR Exchanges Newsletter, No. 56, Vol. 15, No. 2
CMIP5 Experimental Design: Taylor, K.E., R.J. Stouffer, and G.A. Meehl, 2012: An Overview of CMIP5 and the experiment design. *Bull. Amer. Meteor. Soc.*, **93**, 485-498, doi:10.1175/BAMS-D-11-00094.1.
Allen, M. R., and W. J. Ingram, 2002: Constraints on future changes in climate and the hydrologic cycle. *Nature*, **419**, 224-232.
O’Gorman, P. A., and T. Schneider, 2009: The physical basis for increases in precipitation extremes in simulations of 21st-century climate change. *Proc. Natl. Acad. Sci.*, **106**, 14773-14777.
Sun, Y., S. Solomon, A. Dai, and R. W. Portmann, 2007: How often will it rain? *J. Clim.*, **20**, 4801-4818, doi:10.1175/JCLI4263.1.
Wehner, M. F., 2012: Very extreme seasonal precipitation in the NARCCAP ensemble: model performance and projections. *Clim. Dyn.*, doi: 10.1007/s00382-012-1393-1.

HEAVY PRECIPITATION CHANGES

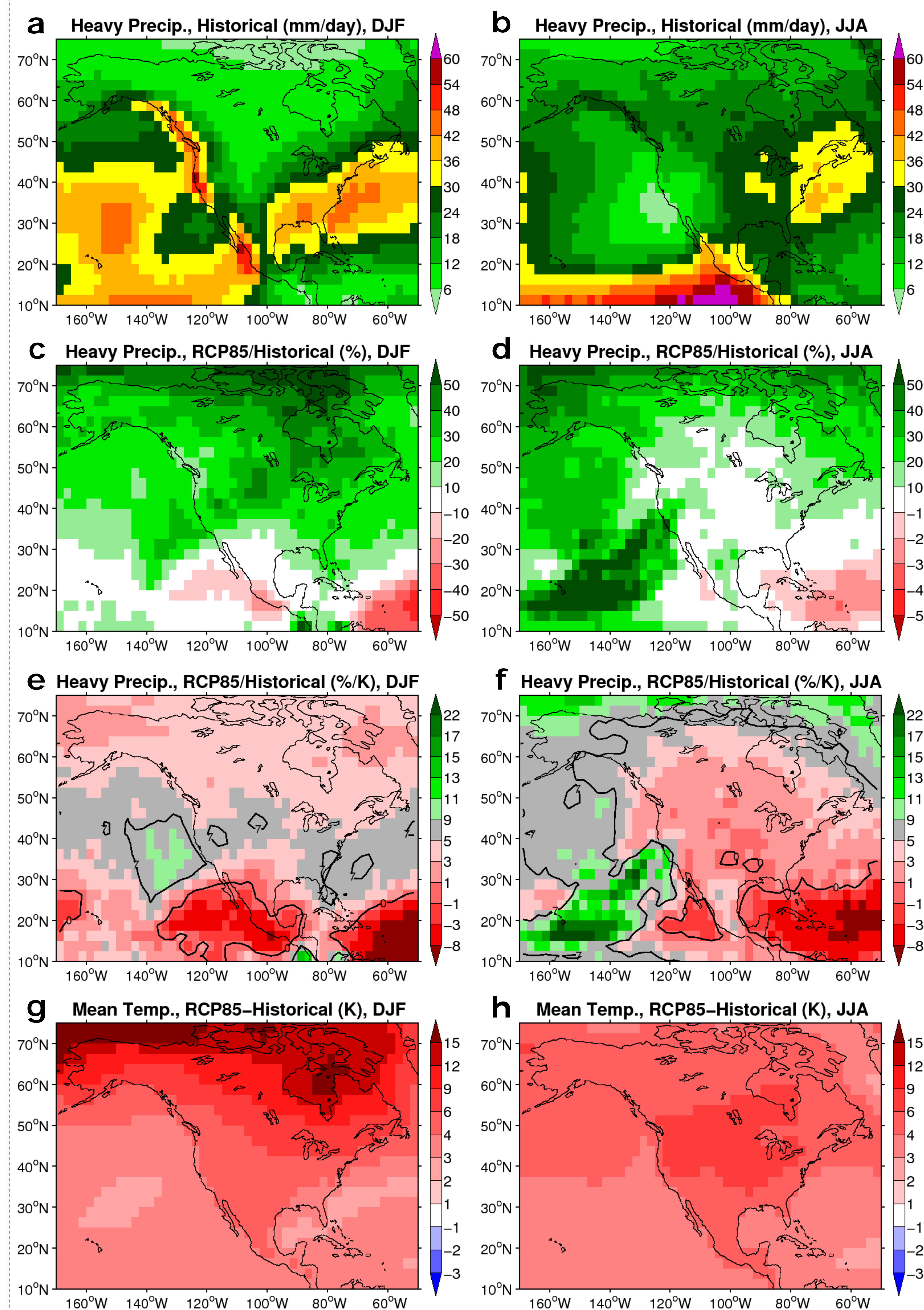


Figure 1. (a,b) Mean precipitation coming from the daily 99th percentile and above (P99M) for the historical simulation. (c,d) The percent change in P99M between the historical and RCP85 simulations. (e,f) Percent change in P99M per locally smoothed mean temperature change. (g,h) Mean temperature change. Left: winter, Right: summer. All panels show the multi-model average.

- In the absence of atmospheric circulation or other changes, increases in extreme precipitation would be expected to coincide with increases in atmospheric water vapor, at approximately 7% per degree of warming.

PHYSICAL MECHANISMS

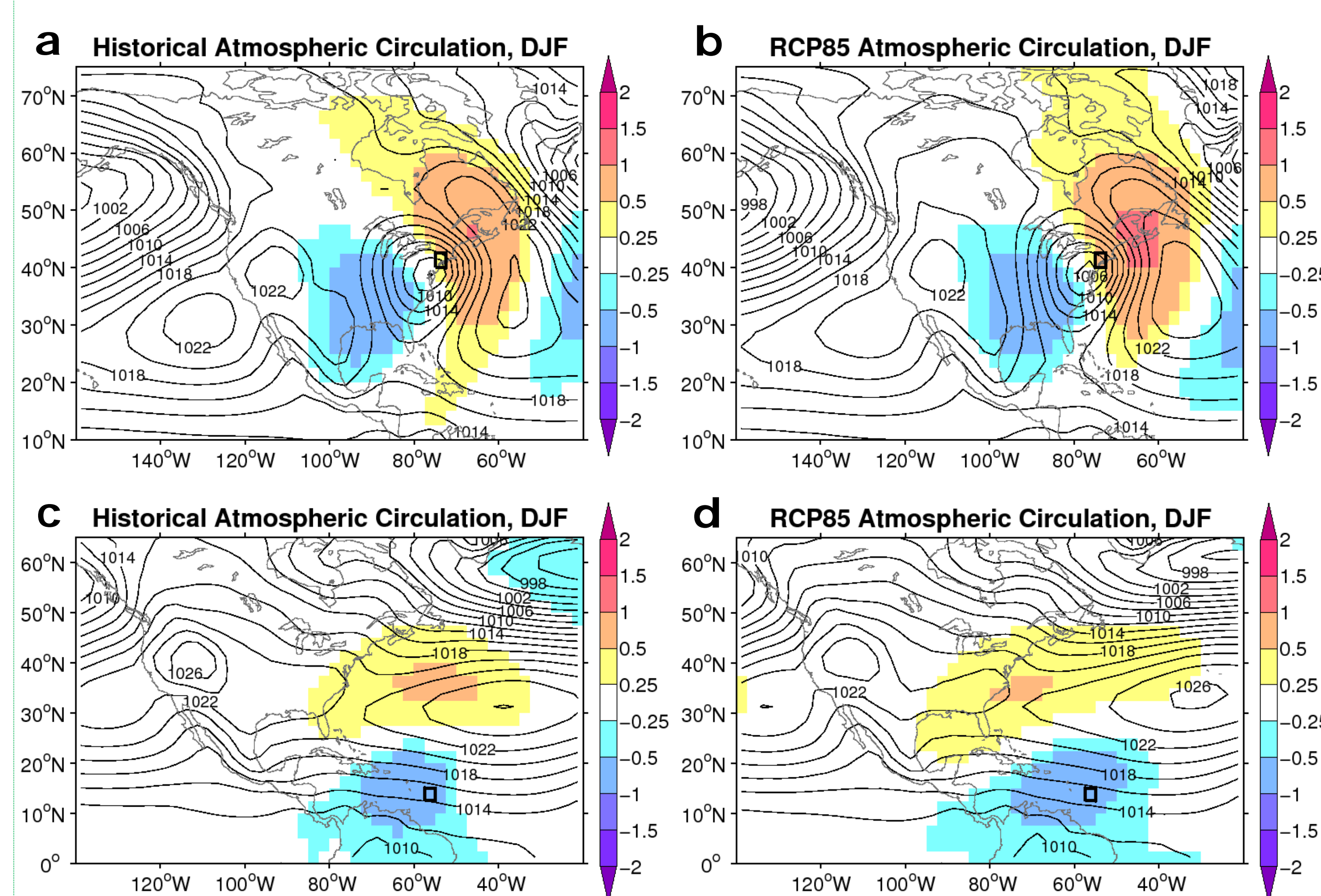


Figure 2. The average sea level pressure (hPa, black contours) and 500 mb geopotential height standardized anomaly (dimensionless, color fills) for the wettest 21 winter days at a grid cell in the (a,b) northeast US and (c,d) Atlantic. The standardized anomalies were computed using a seasonally varying climatology. Left: historical, Right: RCP85. All panels show the multi-model average (17 of total 24 models used).

- The similarity in circulation patterns between the historical and RCP85 scenarios is characteristic of many other locations throughout the domain in addition to those displayed above.
- Climatology or large inter-event variability may be influencing the atmospheric circulation composite patterns at low latitude locations. Further investigation and possibly additional metrics to quantify extreme precipitation mechanisms may be necessary.

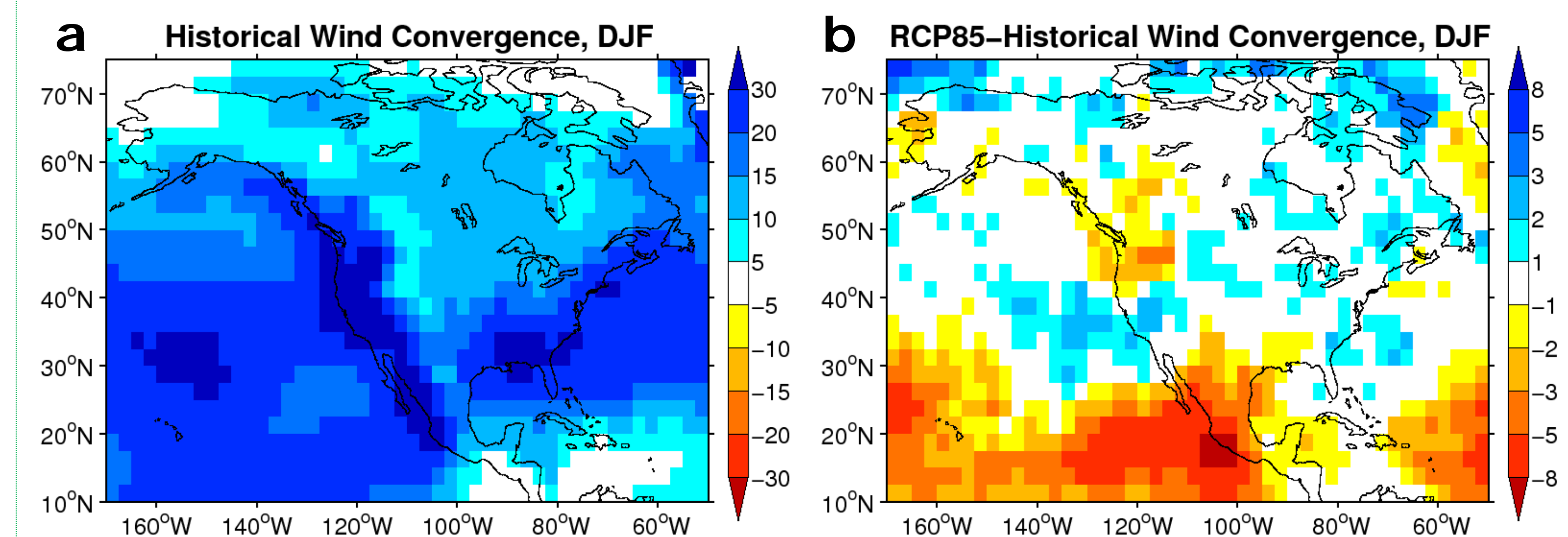


Figure 3. The convergence of the vertically integrated wind (surface–600-mb, $10^{-3} \text{ kg/m}^2/\text{s}$) averaged over the 21 most extreme winter precipitation events at each grid cell on the domain. (a) Historical. (b) Difference between RCP85 and historical. The multi-model average is shown (17 of total 24).

- The convergence of low-level wind is slightly weaker in the RCP85 simulation over regions where heavy precipitation decreases in intensity (see Fig. 1e). This is also the case for extreme summer precipitation events (not shown). These results are interesting and require further exploration.

<u>Modeling Group</u>	<u>Model Name</u>	<u>Lon. (°)</u>	<u>Lat. (°)</u>
Commonwealth Scientific and Industrial Research Organization (CSIRO) and Bureau of Meteorology (BOM) (Australia)	ACCESS1.0	1.88	1.24
Beijing Climate Center, China Meteorological Administration (China)	BCC-CSM1.1*	2.81*	2.81*
College of Global Change and Earth System Science, Beijing Normal University (China)	BNU-ESM	2.81*	2.81*
Canadian Centre for Climate Modelling and Analysis (Canada)	CanESM2*	2.81*	2.81*
National Center for Atmospheric Research (USA)	CCSM4 (r6)	1.25	0.94
Centro Euro-Mediterraneo per I Cambiamenti Climatici (Italy)	CMCC-CM	0.75	0.75
Centre National de Recherches Meteorologiques / Centre Europeen de Recherche et Formation Avancees en Calcul Scientifique (France)	CNRM-CM5*	1.41	1.41
Commonwealth Scientific and Industrial Research Organization in collaboration with Queensland Climate Change Centre of Excellence (Australia)	CSIRO-Mk3.6.0*	1.88	1.88
LASG, Institute of Atmospheric Physics, Chinese Academy of Sciences (China)	FGOALS-s2*	2.81	1.67
NOAA Geophysical Fluid Dynamics Laboratory (USA)	GFDL-ESM2G*	2.50	2.00
	GFDL-ESM2M*	2.50	2.00
Met Office Hadley Centre (UK)	HadGEM2-CC*	1.88	1.25
	HadGEM2-ES	1.88	1.24
Institute for Numerical Mathematics (Russia)	INM-CM4*	2.00	1.50
Institut Pierre-Simon Laplace (France)	IPSL-CM5A-LR*	3.75*	1.88*
	IPSL-CM5A-MR*	2.50	1.26
	IPSL-CM5B-LR	3.75*	1.88*
Atmosphere and Ocean Research Institute (The University of Tokyo), National Institute for Environmental Studies, and Japan Agency for Marine-Earth Science and Technology (Japan)	MIROC5*	1.41	1.41
Japan Agency for Marine-Earth Science and Technology, Atmosphere and Ocean Research Institute (The University of Tokyo), and National Institute for Environmental Studies (Japan)	MIROC-ESM*	2.81*	2.81*
	MIROC-ESM-CHEM*	2.81*	2.81*
Max Planck Institute for Meteorology (Germany)	MPI-ESM-LR*	1.88	1.88
	MPI-ESM-MR*	1.88	1.88
Meteorological Research Institute (Japan)	MRI-CGCM3*	1.13	1.13
Norwegian Climate Centre (Norway)	NorESM1-M	2.50	1.88

List of the CMIP5 models used for analysis in this poster. Asterisks next to the model names indicate the 17 models that were used for the atmospheric circulations analysis (right column on poster) due to output availability. All 24 models were used for the precipitation analysis (middle column on poster). The approximate spatial resolutions (Lon. and Lat. columns) were calculated by dividing 360° or 180° by the number of grid cells in the longitude or latitude dimensions, respectively. Asterisks next to spatial resolution denote climate models whose grids were transformed to the common 2.5°x2.5° lon-lat resolution using linear interpolation. All others were transformed using area averaging. The first ensemble member run (except for the NCAR-CCSM4, in which run 6 was used) was used from each model.